UNIVERSITY
OF
QUEENSLAND

Department of Civil Engineering

RESEARCH REPORT SERIES

Time Dependent Deformation in Prestressed Concrete Girder: Measurement and Prediction

Y.J. SOKAL and P. TYRER

Research Report No. CE30

November, 1981

CIVIL ENGINEERING RESEARCH REPORTS

This report is one of a continuing series of Research Reports published by the Department of Civil Engineering at the University of Queensland. This Department also publishes a continuing series of Bulletins. Lists of recently published titles in both of these series are provided inside the back cover of this report. Requests for copies of any of these documents should be addressed to the Departmental Secretary.

The interpretations and opinions expressed herein are solely those of the author(s). Considerable care has been taken to ensure the accuracy of the material presented. Nevertheless, responsibility for the use of this material rests with the user.

Department of Civil Engineering,
University of Queensland,
St Lucia, Q 4067, Australia,
[Tel:(07) 377-3342, Telex:UNIVQLD AA40315]

TIME DEPENDENT DEFORMATION IN PRESTRESSED CONCRETE GIRDER: MEASUREMENT AND PREDICTION

by

Y.J. Sokal, BSc, MSc, DSc, MASCE
Lecturer in Civil Engineering

and

P. Tyrer, BE
Engineer, Leighton Contractors, Pty Ltd, Queensland

RESEARCH REPORT NO. CE 30
Department of Civil Engineering
University of Queensland
November, 1981

Synopsis

Prestressed concrete girders which are intended for composite construction in bridges and other similar structures are often stored unloaded for some time before being placed in their final positions where top deck is being poured over.

During that free storage the girders are subjected to creep and shrinkage which manifests itself through increased upward deformation usually defined as camber. The analytical estimation of this deformation is important as it controls the minimum thickness of the top deck. If this deformation is exagerated, then this requires increase of the top deck and possible change in the level of bridge surface. The estimation of creep deformation is made generally in a single step calculation using data from applicable standards.

In this paper an attempt was made to correlate on site measurements with continuous computer modelling of the time-dependent behaviour using data from recently adopted international standard for concrete structures. It was found that computer modelling does predict faithfully the general behaviour of the girder. However, data from the herein used international standard is exagerated for local conditions, so that the completed camber was larger than the measured one.

CONTENTS

DON '62

FRYER.

1. INTRODUCTION

The paper describes the investigation of the camber deflection of a simply supported precast prestressed concrete girder intended for a composite concrete highway viaduct bridge over Bramble Bay crossing in Brisbane, Queensland. The purpose of the investigation was to measure the development of camber with time and to assess how successfully it can be predicted by computer simulation.

The girder had a constant I-section and was prestressed with forty-four 12.7 mm diameter 7-wire strands of which thirty-four were draped symmetrically about the centre of the span. The details of the girder are shown in Figure 1. It was manufactured on a site close to the bridge crossing. The manufacturing process allowed production of two identical girders in three days, except when interrupted by weekends and holidays. The bridge authority (Main Roads Department, Brisbane) and the contractor (Barclay Brothers Pty Ltd, also from Brisbane) allowed storage of one particular girder on a location where it could be easily accessed for a sufficient length of time to carry out the investigation.

The casting history of the girder was as follows:

Day 1 Reinforcement is placed in forms for two girders placed end to end. The prestressing reinforcement is continuous throughout (Fig. 2) and the prestressing is achieved by pushing one of the forms away from the other while the prestressing force is controlled by the increase in the gap between the two girders (Fig. 3).

Day 2 Pouring of ready mixed concrete and compaction by internal and external vibration. Low pressure steam curing at 70° starts immediately after compaction and lasts

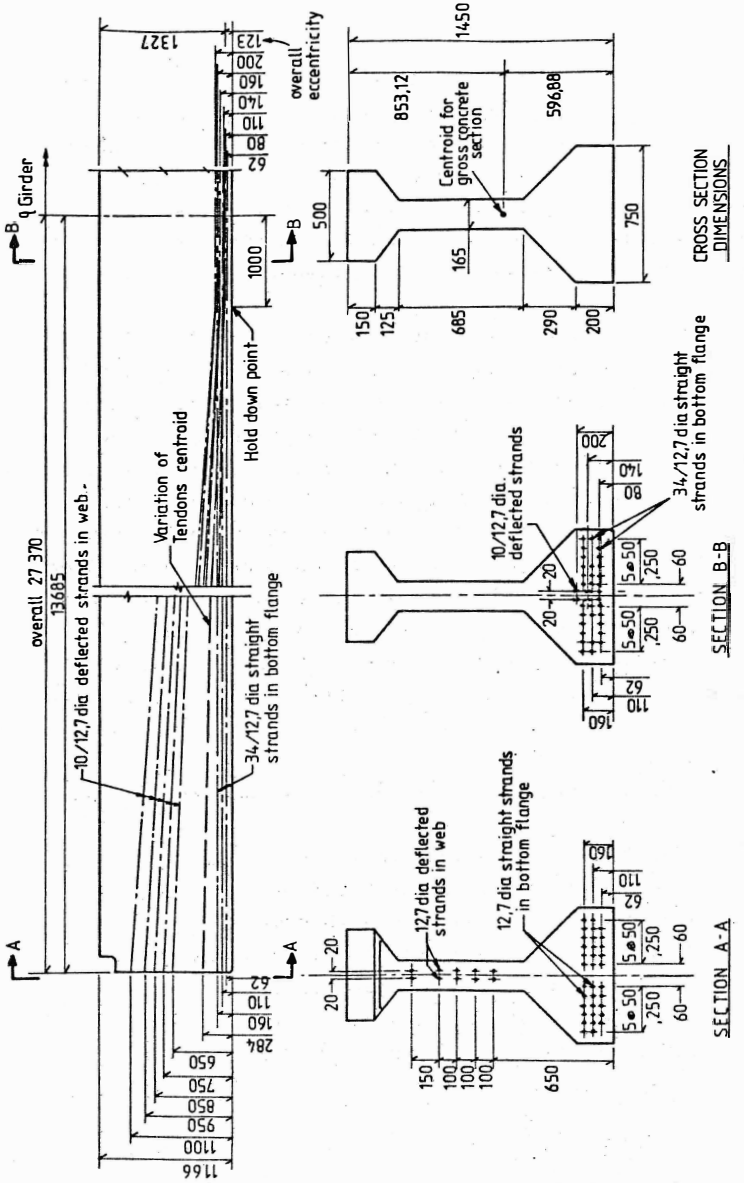

FIGURE 1 : Details of the investigated girder

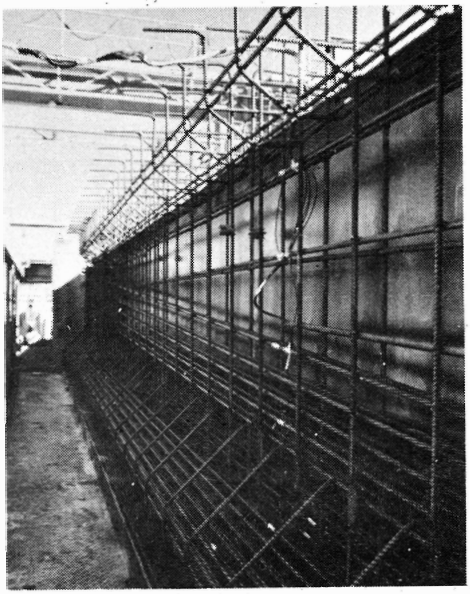

FIGURE 2 : Reinforcement of the girder

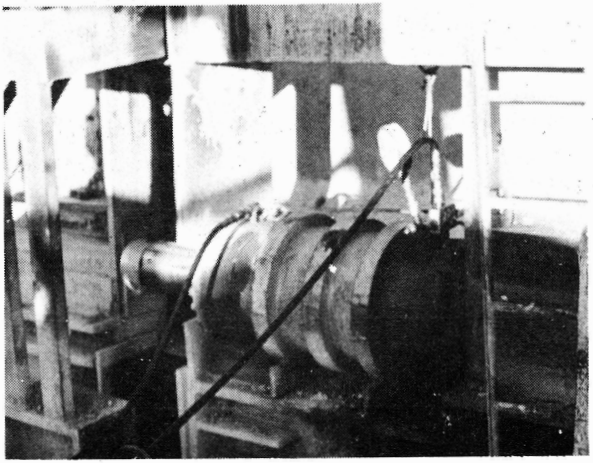

FIGURE 3 : Prestressing jacks

twelve hours. The time-temperature curve for steam curing is shown in Fig 4.

Day 3 Release of prestress (the transfer) approximately seven hours after stoppage of the steam supply and transportation to the temporary storage one hour later. During the transportation the beam was suspended at both ends (Fig. 5) which means that the statical system was not affected.

The detailed timetable is shown in Table 1.

2. MATERIALS

Concrete from identical mixes has been previously thoroughly investigated on the site (2) and the main results obtained are reported in Table 2 below.

The composition of the concrete is given in Appendix I. The concrete has been tested at different ages for compressive strength and for secant modulus of longitudinal deformation (modulus of elasticity). Tested cylinders were subjected to the same curing regime as the girder.

Strands were uncoated 7-wire stress-relieved with special low-relaxation properties. They were supplied with specifications for breaking strength, Ø.2% proof stress, modulus of elasticity and the ultimate elongation for a specified length. The average values from ten specimens are presented in Table 3.

In the girder strands were pretensioned to 80% of the breaking strength.

Strands were tested (7) in the laboratory, without surrounding concrete, in a specialy designed rig, which

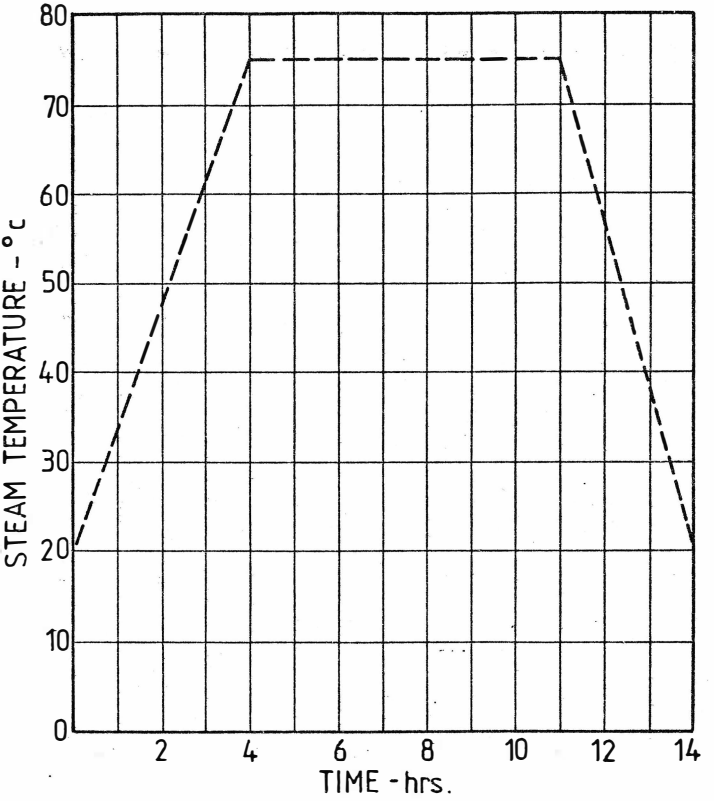

FIGURE 4 : Steam curing curve

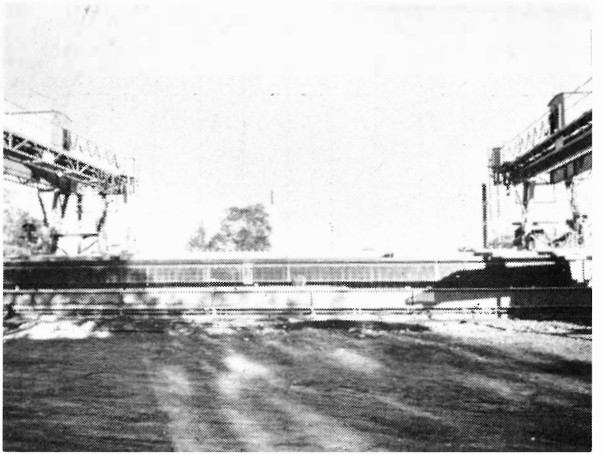

FIGURE 5 : Transportation of the girder

TABLE 1 : General Timetable of the Investigation

Date	Time Counted from Release of Prestress		Manufacturing Action	Deflection Measurement
	Days	Hours		
21.4.79	-3	-70	Placing of reinforcement, prestressing, placing of forms	
23.4.79	-1	-21	Pouring of concrete and compaction	
		-19 to -7	Steam curing (12 hours)	
24.4.79		-1		Yes
	0	0	Release of prestress (transfer)	Yes
		1	Transportation to the permanent location	
		1.5		Yes
28.4.79	4			Yes
2.5.79	8			Yes
5.5.79	11			Yes
9.5.79	15			Yes
16.5.79	22			Yes
23.5.79	29			Yes
26.5.79	63			Yes

TABLE 2 (2) : Tested Concrete Properties

Time After Compaction Days	Properties of Concrete	
	Compression Strength MPa	Secant Modulus of Elasticity GPa
1	36.6	27.3
7	43.6	27.6
28	46.4	29.3
90	51.3	30.8

TABLE 3 (7) : Properties of Strands

Item	Value
Modulus of elasticity	190.3 GPa
Breaking strength	192.5 kN
Steel area	98.84 mm
Proof load at 0.2% elongation	179.27 kN
Elongation in 24" (610 mm) length	6.61 %

consisted mainly of two rigid and fixed plates to which strands were pretensioned. Relaxation was measured with calibrated precision load cell. The initial tension varied between Ø.8 and Ø.7 of the breaking strength. The main conclusions from tests as reported in (7) were as follows:

- relaxation at constant and normal temperature prior to steam curing can be calculated from the equation

$$R = 2.7 + Ø.7 \log t$$

  where R is expressed in percent of initial tension and logt is the decimal logarithm of time t in hours counted from the time of prestressing;

- net relaxation due to steam curing was 5.94% of the initial tension;

- there was no relaxation after steam curing.

For the purpose of the girder analysis, total relaxation was calculated as follows:

Relaxation in 51 hours prior to steam curing	$R = 2.7 + Ø.7 \log 51$	= 3.9
Relaxation during steam curing		= 5.94
	Total relaxation	= 9.84

This value is judged to be reliable despite the difference in the time of curing (six hours in the laboratory, twelve hours on site). In fact, it is shown in (7) and also in (1Ø) and (11) that most of the curing relaxation happens during the first hours of the process.

3. EXPERIMENTAL INVESTIGATION

This included:

(a) measurement of the deflection along the top surface of the girder;

(b) measurement of temperature variation across several vertical sections within the girder.

3.1 Measurement of Deflections

Special bolts were inserted into the top of the beam at appproximately eight points along the span during pouring of concrete. These bolts protruded above the concrete surface and were anchored in concrete with three welded blades spread horizontally in different directions. The protuding ends were ball shaped to allow easy positioning of a surveying staff. The measurements were made with the help of a surveying level which gave overall accuracy of Ø.1 mm. This arrangement allowed measurement of deflections relative to end supports, thus eliminating the necessity to control any setlements there. The positioning of bolts in shown in Figure 6. The method of calculating deflections from numbers read on the surveying staff is also shown in that figure.

The first measurement of deflections was done prior to transfer of prestress, i.e. at - Ø1 hours. The second measurement was made immediately after the transfer and this was again followed by measurement after the girder had been transported to its temporary location, about one hour after transfer of prestress. It is assumed that the transportation itself as shown in Fig. 5 had no effect on the deflected shape. Subsequent measurements were taken at several days intervals for the whole time of the investigation which was 35 days.

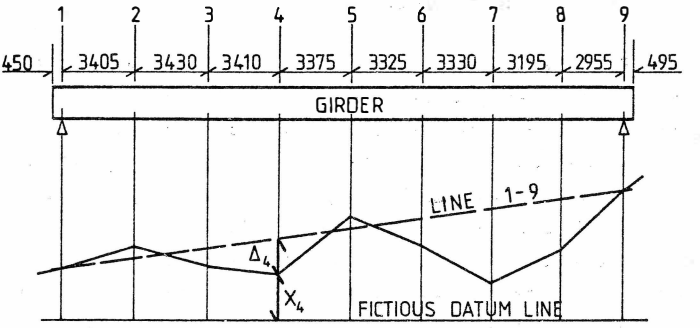

IF X_i, is the measured value on the surveying staff at point i, than the deflection of point i relative to the straight line between point 1 and 9 is:

$$\Delta_i = X_i - \left[X_1 + \frac{X_9 - X_1}{8} (i-1) \right] \quad \text{(positive above line 1-9)}$$

FIGURE 6 : Method of measuring deflections of the girder top

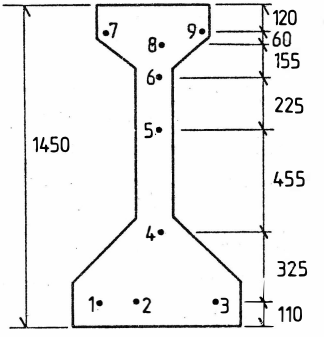

FIGURE 7 : Arrangement of thermocouples in the cross-section

3.2 Measurement of Temperatures

For the purpose of temperature measurement three sections at quarter points along the girder span were instrumented with thermocouples. Each section contained nine thermocouples. The typical arrangement is shown in Figure 7. The thermocouples were made from copper and constantin wires Ø.558 mm diameter soldered together at the measuring point. From the measuring point copper wire extended to a reading instrument (digital voltmeter), while constantin wire extended to a reference junction maintained at Ø°C with the help of ice. Another copper wire jointed the reference junction with reading instrument. The output was read in milli-volts and was translated into temperature in degrees Celsius, with the help of a standard calibration chart. Typical temperature gradients are shown in Figure 9.

Because of the limited number of measured curvatures, it was assumed for the purpose of calculation of deflections that curvatures are constant between centre points of instrumented sections. The possibility of using this approximation was confirmed from the measured data, which shows similar variations and similar magnitudes in all three measured sections. However, it must be kept in mind that the possibility of omitting some temperatures which could have some contributions should not be excluded.

At early age the girder has been heated to approximately 75°C during curing and because of the duration of the curing, it is assumed that this temperature has been uniformly distributed throughout the girder.

In the time which followed curing, the girder was subjected to differential cooling which was faster in the upper part. When the temperature within the girder reached the status quo (after disappearance of the curing effects), the temperature variation was controlled by exposure to sun rays and to ambient temperature. At early stages the temperature differential caused by curing resulted in sagging deformations, while heating of the top in the late

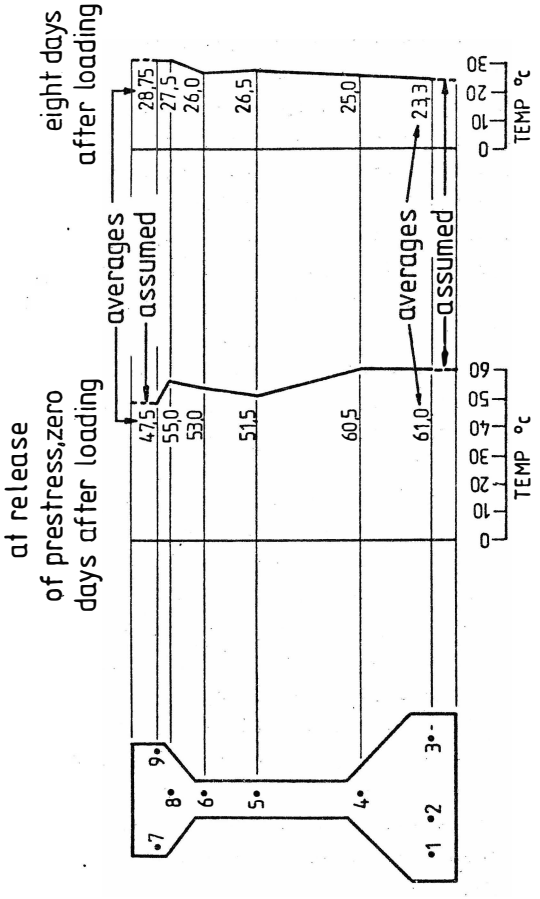

FIGURE 8 : Typical temperature distribution

stages resulted in hogging deformations which added to the creep and shrinkage camber.

4. CALCULATION OF DEFORMATIONS CAUSED BY TEMPERATURES (5)

The change in the girder temperature affected both longitudinal and vertical deformations. For the purpose of the analysis of deformation, any non-uniform temperature distribution across a vertical section (relative to a certain datum) may be decomposed into three components as shown in Figure 9. The AVERAGE component is uniform throughout the section and is responsible for longitudinal deformation, the LINEAR component is responsible for the generation of curvatures which integrate into vertical deflection or camber and the NON-LINEAR component is responsible for residual stresses.

The girder hardened at a temperature of around 70° C, while the ambient temperature was much lower (15°C - 25° C). Even with some cooling, the beam could not deform from the temperature effect before release of prestress because of restraint provided by anchored strands and steel forms. As mentioned earlier, it was assumed that at the time of the first deflection measurements (before transfer), the temperature was uniform throughout and equal to 70°C. This assumption is further supported by the fact that after discontinuation of the steam supply, the girder remained for a while in the steel forms which served as heat insulators. The calculated temperature corrections and the measured camber are shown in Table 10.

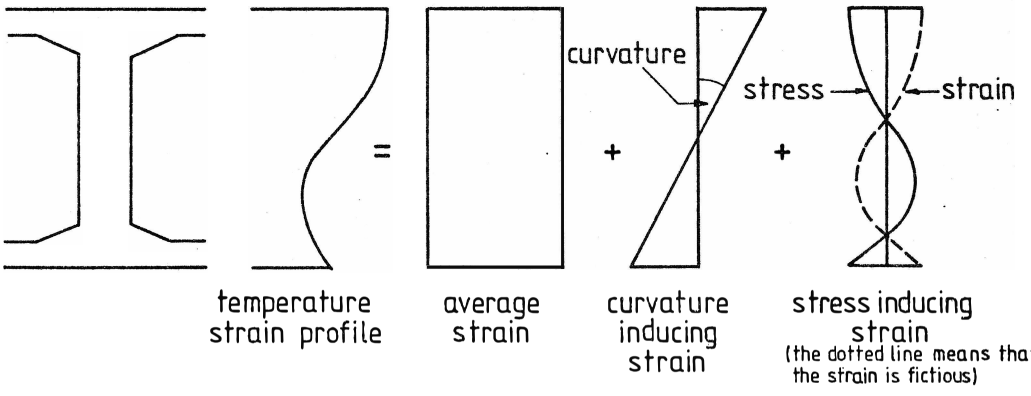

FIGURE 9 : Decomposition of temperature stress for the purpose of analysis (5)

5. ANALYTICAL INVESTIGATIONS FOR CREEP AND SHRINKAGE EFFECTS

The aim of these analytical investigations is to calculate the changes in the deformed shape of the girder with time as affected by creep and shrinkage. Creep and shrinkage cause change in strain distributions which in turn cause redistribution of stresses. The deformed shape is calculated from curvatures which are calculated through integration of strains at discrete equidistant sections of the girder.

The calculations require information on three concrete parameters: modulus of deformation (modulus of elasticity) creep and shrinkage. All three parameters are time dependent.

5.1 Data on Modulus of Elasticity, Creep and Shrinkage

The curve for the variation of the modulus of elasticity with time was obtained by using the four available experimental data points (Table 2). This curve is presented on Figure 10.

Standard curves for creep and shrinkage from CEB Model Code (3) were used as it was considered that this code contains contributions from the largest scientific community. At the time of writing this report these curves were available only in graphical form on a semi-log scale. The required curves from graphs were read at as many discrete points as accurately as the logarithmic scale allowed it. These discrete values were then used directly in the computer program as discrete data. At the same time analytical expressions were derived which closely correlated with curves drawn through discrete points. Another computer program was developed which used the derived analytical expressions. The quantitative implementation of shrinkage and creep coefficients is detailed in Appendix II and the measured and derived curves are shown in Figs. 11, 12 and 13.

It is shown in details in Appendix II that the creep deformation accordingly with CEB Code is the sum of three components: reversible deformation (or delayed elasticity), irreversible deformation or flow and an odd single component of the irreversible deformation which occurs during the first day of loading. The shrinkage deformation in the CEB Code is presented by a one component only. The CEB data is intended to be used in the SUPERPOSITION method of analysis. However, in this investigation it has been implemented in a discretised RATE-OF-CREEP method of analysis. Both methods are explained in References (4), (6), (8) and (11). For the sake of clarity and to emphasize the differences between the two methods and the difficulties, in the implementation, the major features in both methods are outlined below.

In the discretised SUPERPOSITION METHOD the time of integration is divided into finite steps and for each step additional shrinkage and creep strains in a particular section of the girder are calculated from stress magnitudes there. These additional strains inevitably cause changes in stresses and each incremental (or decremental) stress must be treated as a newly applied stress with different creep and strain histories. It can be now easily realised that N time steps will require N stress histories to be dealt with and superimposed together.

In the discretised RATE-OF-CREEP method the first time step is dealt with in exactly the same manner as in the SUPERPOSITION method, but here the similarity ends, because creep and shrinkage increments for the second and all successive time steps are calculated using creep and shrinkage curves for the first step. This means that instead of N time histories, there are only one creep and one shrinkage histories for different stress distributions at each time step.

The discretised RATE-OF-CREEP method has been used here in two computer programmes. One program used discrete

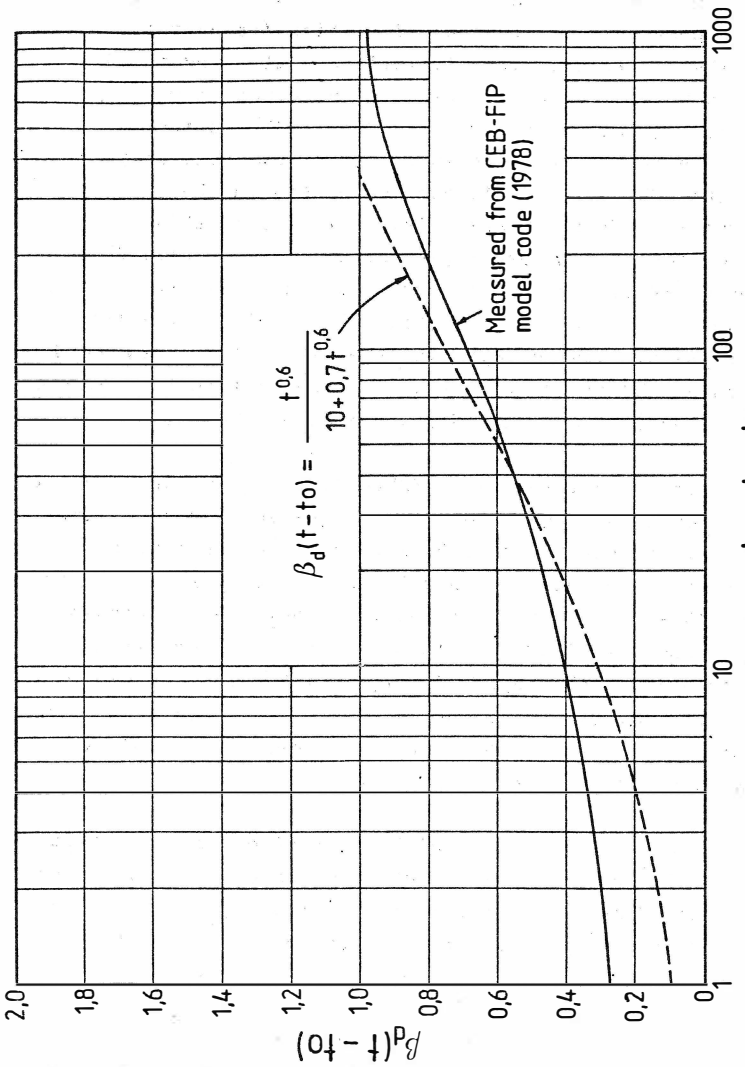

FIGURE 10 : Modulus of elasticity for concrete

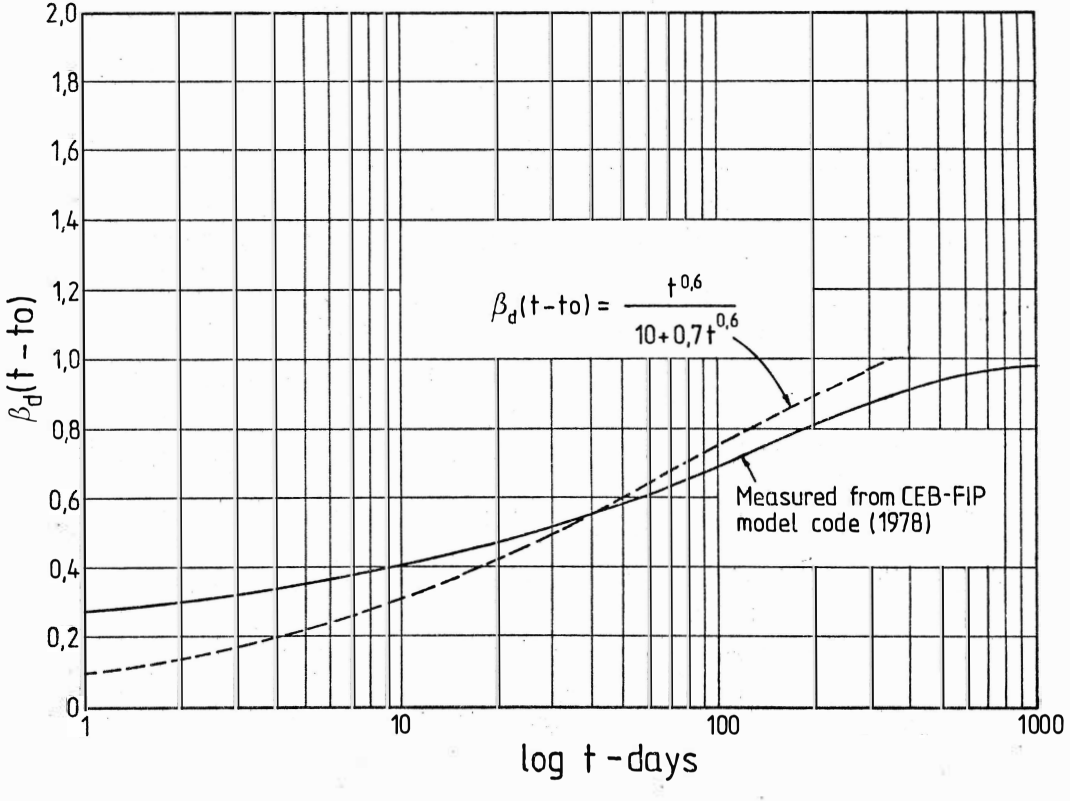

FIGURE 11 : β_d creep coefficient

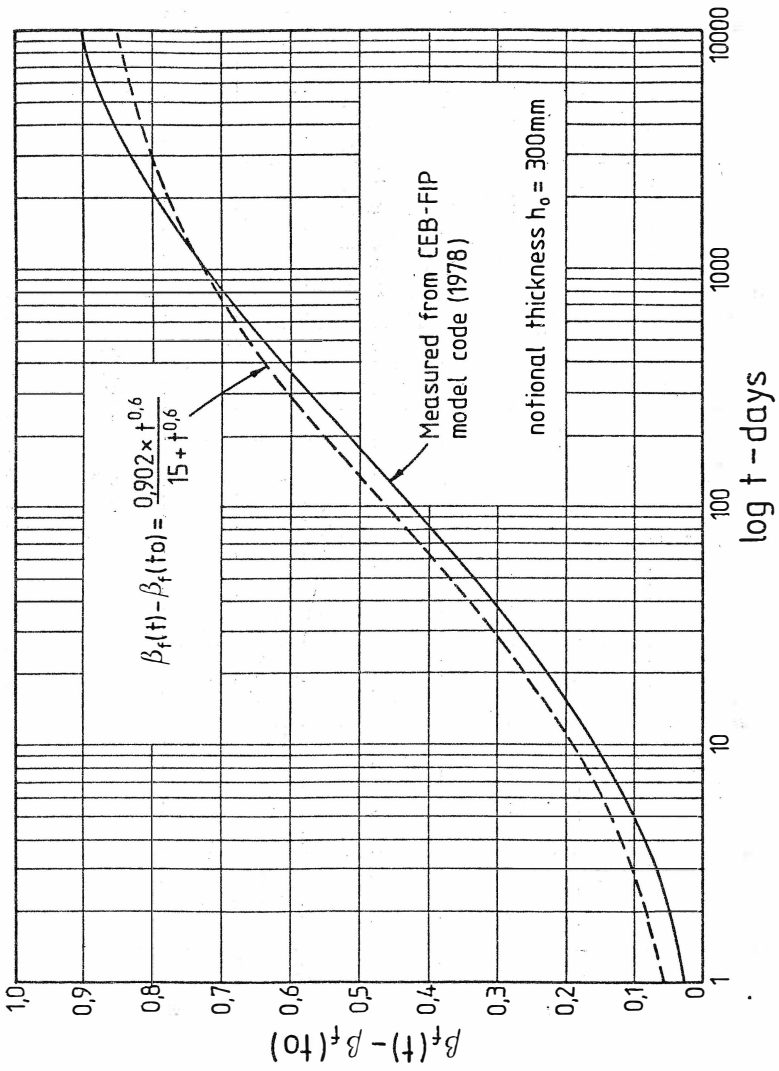

FIGURE 12 : β_f creep coefficient

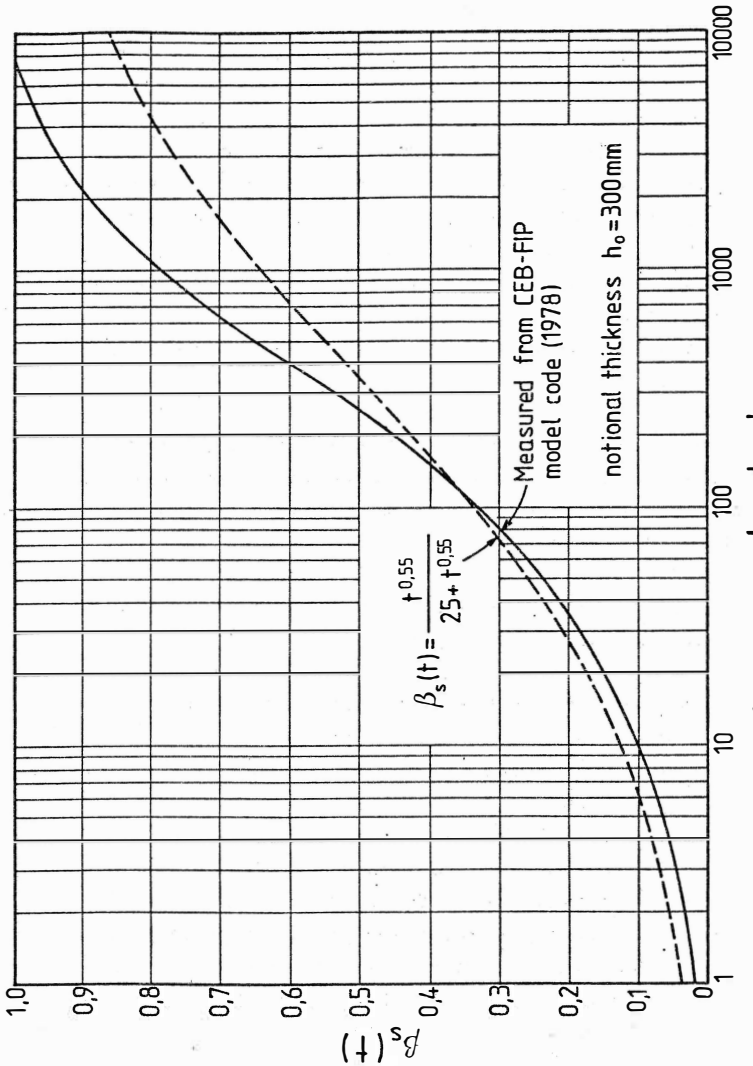

FIGURE 13 : β_s shrinkage coefficient

data read directly from CEB graphs while the second program used derived analytical expressions.

5.2 Implementation of the Rate-of-Creep Method (8)

Basic assumptions:

- linear creep
- perfect bond between prestressing tendon and concrete
- at a particular section all tendons are assumed to act at the common centroid
- distribution of stresses and strain across sections is linear
- the girder is symmetrical about the centre of the span.

The girder length is divided into arbitrary even number of segments with equal length and the girder properties are assumed to be concentrated at intersections between segments, called stations.

The following procedure is repeated for each station in one half of the span:

Step 1 At the time of transfer calculation of:
(a) instantaneous loss of prestress
(b) stresses and strains in concrete.

Step 2 Time is incremented by the length of the integration time step and the following calculations are performed successively:
(a) incremental creep and shrinkage strains at top and bottom of the section;
(b) adjustment of stresses and strains in concrete to preserve linear distribution of strains and equilibrium of stresses;
(c) incremental creep and shrinkage strain at centroid of prestressing strands and the resulting loss of prestress;
(d) adjustment of stresses and strains in concrete

resulting from the loss of prestress.

Step 2 is then repeated for all subsequent time intervals.

5.3 Curvatures

At the end of each time step the curvatures at a station are equal to the difference of strains at top and bottom divided by the section height. With curvatures available at each station the deflection at any point can be calculated using the conjugate beam method, i.e. assuming that the curvatures are discrete loads and that the bending moments resulting from these loads are the deflections.

6. TESTING OF THE GENERAL PERFORMANCE OF COMPUTER PROGRAMS

As mentioned earlier, calculation of time dependent changes (like creep and shrinkage) was performed using two different data inputs. In the first input, data on shrinkage and creep were read discretely from CEB graphs and here all data points may be asumed correct within the direct reading accuracy. Not so in the program where data is calculated from analytical formulae which give values which deviate slightly from the CEB values. However, the program with analytical formulae has certain computational advantages over the other program because it offers, among others, flexibility in the choice of the length of the integration time step and this allows testing for the effects of this parameter.

In general the computational efficiency is governed by two parameters: length of the integration time step and number of sections for which calculations are performed. The length of the integration time step is the most important parameter since it controls the development of strains and stresses and consequently curvatures in each section, while the precision in the integration of

curvatures is controlled by the number of sections.

The program with analytical formulae had two variations. In one variation the length of the integration time step was uniform for defined time periods and in the second it formed a geometric ascending progression. Table 4 gives detail of all three programs.

a. Test for the effect of number of segments

Program A (with discrete and more accurate data input) was executed using different number of sections (segments). Total length of integration was kept constant and equal to 100 days. The effect on deflection is shown in Table 5.

Table 5 shows the obvious conclusion that a very small number of sections is required to achieve accuracy. This happens because the deflection is superimposed from deflections caused by a uniformly distributed load and by prestressing strands with an eccentricity which has an almost constant rate of change along the girder span. Both the uniformly distributed load and the prestressing strands produce parabolic deflection (prestressing strands produce higher degree parabola) and since the integration uses Simpson's rule three sections (two segments) in the half span of the symmetric girder give almost sufficient accuracy. Substantial reduction in the number of segments causes reduction in magnitude of the central deflection. All subsequent calculations use 40 segments.

b. Comparison between Programs A and B1

Programs A and B1 were executed using identical time steps. Comparison of relative camber end of loss of prestress is shown in Table 6.

The conclusion from Table 6 is that program B1

TABLE 4 : Integration Step Length in the Used Programs

PROGRAM A: Discretely Input Data		PROGRAMS B: Input Data Computed Analytically		
		B 1		B 2
Length of Integration (Days)	Integration Step Length (Days)	Length of Integration (Days)	Integration Step Length (Days)	Integration Step Length is a Geometrical Progression where QU is Progression Factor
1-10	1			
10-100	10	1-100	any	$t_N - t_{N-1} = t_N \left(\frac{QU-1}{QU}\right)$ QU > 1
100-1000	100	100-1000	any	
1000-10000	1000	1000-10000	any	$t_N = t_{N-1} \times QU$

TABLE 5 : Effect of Number of Segments on Camber at Mid-Span Section

Number of Segments	Relative Camber at Day After Loading								
	0	1	5	10	20	40	60	80	100
400	1.0	1.0	1.0	1.0	1.0	1.0	1.0	1.0	1.0
200	1.0	1.0	1.0	1.0	1.0	1.0	1.0	1.0	1.0
80	1.0	1.0	1.0	1.0	1.0	1.0	1.0	1.0	1.0
40	1.0	1.0	1.0	1.0	1.0	1.0	1.0	1.0	1.0
20	1.0	1.0	1.0	1.0	1.0	1.0	1.0	1.0	1.0
16	1.0	1.0	1.0	1.0	1.0	1.0	1.0	1.0	1.0
12	1.0	1.0	1.0	1.0	1.0	1.0	1.0	1.0	1.0
8	.997	.996	.997	.995	.988	.996	.996	.996	.996
4	.989	.988	.988	.989	.988	.988	.989	.988	.992

TABLE 6 : Comparison Betweeen Programs A and B1 Using the Same Source Data. Both Programs Use 40 Segments

Program	Relative Camber at Day After Loading					
	10	100	500	1000	5000	10000
Program A	1.0	1.0	1.0	1.0	1.0	1.0
Program B1	0.88	0.90	0.90	0.89	0.87	0.87
	Loss in Prestress (per cent)					
Program A		1.00			1.00	1.00
Program B1		1.12			1.05	1.03

gives larger loss of prestress and therefore gives smaller camber. This difference is certainly due to inaccurate analytical interpretation of the discretely read data in program B1.

c. Test for the effect of the length of the integration time step

Programs B1 and B2 were used to test the effect of time step on camber at centre of span and on loss of prestress in the central section. The effect on camber is shown in Table 7 where the camber at a certain time is presented in its relative value to the camber calculated when the integration step length is as follows: one day for the first 1000 days and 10 days for the remaining 9000 days.

It can be concluded from Table 7 that increase in integration step length in program B1 increases central deflection. The error is maximum at 100 days and decreases subsequently for longer integration length. Integration step length in program A gives sufficient accuracy. Program B2 gives sufficient accuracy even with relatively large progression factor (QU = 1.7) for the first 1000 days, however, error increases substantially later.

The loss of prestress is less affected by the change in the step length and large steps (up to 100 days) gave sufficient accuracy as is shown in Table 8.

The difference between the effects on camber and on prestress results from the fact that curvature is controlled by the difference in strains on the opposite sides of the section (top and bottom) while loss in prestress is controlled by the change in strains at centroid of strands. The stress on top of the section being different than the stress at bottom of the section, the creep effect causes strains at top and at bottom to develop at constantly diverging rate.

d. Effect of shrinkage magnitude

Program A was used to test the effect of shrinkage on final deflection and on loss of prestress. For that purpose the shrinkage strain (see Appendix II) varied between 0.00015 and 0.0004. Overall the effect is small; however, it increases substantially with time. Table 9 shows the reduction in camber and the increase in loss in prestress for different times when shrinkage strain varies.

Table 9 suggests two obvious conclusions:

- larger shrinkage gives larger loss of prestress and therefore smaller camber;

- the difference between the effects of the two chosen shrinkage values increases with time.

7. COMPARISON OF MEASURED AND CALCULATED CAMBER

The measured camber values with and without temperature correction are presented in Table 10 and in Fig. 14. The temperature corrected measured camber is compared with the calculated camber using program A.

The calculated values are too high even with reduction or with total elimination of the coefficient β_a (single component of the irreversible creep deformation). Further reduction of the calculated camber is possible only through reduction of the following:

(a) irreversible creep components ϕ_f and
(b) reversible creep component ϕ_d

This will mean the assumption of humidities larger than 80% (see Appendix II). In view of the relatively dry season during which measurements were made, such large humidity is improbable.

TABLE 7 : Effect of Integration Step Length on Camber

PROGRAM B1						
Length of Integration Steps (Days)	Relative Camber at Day After Loading					
	25	50	100	500	1000	10 000
1*	1.00	1.00	1.00	1.00	1.00	1.00
2*	1.00	1.00	1.00	1.00	1.00	1.00
5*	1.01	1.01	1.00	1.00	1.00	1.00
10	1.01	1.01	1.01	1.01	1.01	1.01
25	1.04	1.03	1.03	1.02	1.02	1.02
50		1.05	1.05	1.04	1.04	1.04
100			1.08	1.07	1.06	1.06
as in Program A			1.00	1.01	1.00	1.01

PROGRAM B2						
Length of Integration Steps (Days)	Relative Camber at Day After Loading					
	25	50	100	500	1000	10 000
QU = 1.15			1.00		1.01	1.03
1.18			1.00		1.01	1.03
1.25			1.00		1.01	1.03
1.35			1.00		1.02	1.04
1.50			1.01		1.02	1.04
1.70			1.01		1.02	1.04

* Integration step length after 1000 days is 10 days

TABLE 8 : Effect of Integration Step Length on Loss of Prestress

PROGRAM B1						
Length of Integration Step (Days)	Loss of Prestress at Day After Loading					
	25	50	100	500	1000	10 000
1*	1.00	1.00	1.00	1.00	1.00	1.00
2*		1.00	1.00	1.00	1.00	1.00
5*	1.00	1.00	1.00	1.00	1.00	1.00
10		1.01	1.01	1.01	1.00	1.00
20			1.01			
25	1.01	1.01		1.01	1.01	1.01
50		1.02		1.02	1.02	1.01
100			1.03		1.03	1.02
as in Program A			1.00	1.00	1.00	1.00

PROGRAM B2						
Length of Integration Step (Days)	Relative Loss of Prestress at Day After Loading					
	25	50	100	500	1000	10 000
QU = 1.15			1.00		1.01	1.04
1.18			1.00		1.01	1.04
1.25			1.00		1.01	1.04
1.35			1.00		1.01	1.04
1.50			1.00		1.01	1.04
1.70			1.00		1.01	1.04

* Integration step length after 1000 days is 10 days

TABLE 9 : Effect of Shrinkage Magnitude on Mid-Span Camber and Loss of Prestress

Reduction of the Mid-Span Deflection when Shrinkage Changes from $\varepsilon_{so} = 1.5 \times 10^{-4}$ to $\varepsilon_{so} = 4.0 \times 10^{-4}$ at Day After Curing				
	100	500	1000	10 000
in percent	0.4	0.8	1.1	2.6
relative to reduction at 100 days	1.0	2.0	2.75	6.50

Increase in Loss of Prestress when Shrinkage Changes from $\varepsilon_{so} = 1.5 \times 10^{-4}$ to $\varepsilon_{so} = 4.0 \times 10^{-4}$ at Day After Curing				
	100	500	1000	10 000
in percent	101.2	102.9	104.9	109.2
relative to loss at 100 days	1.00	1.02	1.04	1.08

TABLE 10 : Mid-Span Measured Camber and Calculated Temperature Deflection (13)

Time in Days from Release of Prestress	Mid-Span Deflection in mm Upward (camber) is Positive Downward Deflection is Negative		
	Measured	Calculated from temperature only	Measured with temperature adjustment
0	27	- 9.9	36.9
4	44.5	1.5	43.0
8	50.6	5.5	45.1
11	47.5	1.8	45.7
15	50.9	5.1	45.8
22	49.7	2.3	47.4
29	50.1	2.5	47.6
63	55.8	3.9	51.9

There is good agreement between the measured and calculated initial camber at transfer. This shows that the initial prestressing force and the modulus of elasticity are correct.

The main cause of discrepancy stems from the higher rate of creep increase for the calculated camber during the first days after the release of prestress which is due to the high rate of creep increase in the CEB data. After approximately ten first days the measured and the calculated camber curves become almost parallel.

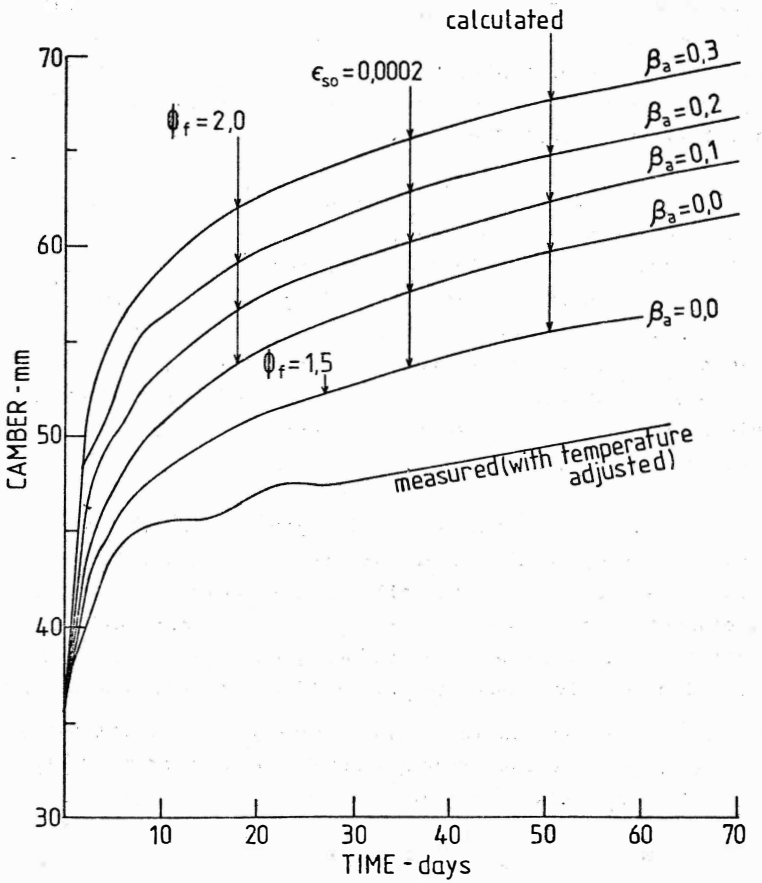

FIGURE 14 : Calculated and measured mid-span camber versus time

8. CONCLUSIONS

A prestressed concrete girder has been used to analyse the development of camber under the action of dead weight and prestress. The camber has been measured on the site and simulated analytically by a discrete integration algorithm developed herein using basic creep and shrinkage data from the recent CEB Code (3).

It is shown that for the particular environmental conditions in which the girder was stored during measurements CEB data gives exaggerated camber. This exaggeration is due mainly to the high rate of creep increase in the CEB data during the first ten days of loading. As shown in Appendix III creep values obtained from Australian Standard (1) are much lower than CEB values. This suggests that the use of data from Australian Standard could give more realistic prediction in this case.

The performance of the integration algorithm was assessed through a series of calculations in which main parameters varied systematically. The conclusion from this assessment is that it is sufficient to input data at discrete times and that the frequency of data input may be reduced successively as the integration progresses away from the time of first loading. The accuracy and the frequency of data input obtained through simple reading from curves given in standards is sufficient.

Computer simulation of time dependent deformation in prestressed girders is possible provided that convergency of solution is checked for the effect of the time main parameters: number of segments and length of the integration time step.

9. ACKNOWLEDGEMENTS

To Main Roads Department and to Barclay Brothers Pty Ltd, both of Brisbane, for allowing this project to be carried out on their construction site.

This paper is based on work by students P. Tyrer and J. McEvoy (13) for their undergraduate thesis project in 1979 under the supervision of Y. Sokal. P. Tyrer aassisted in the writing of the paper.

APPENDIX I - MATERIAL PROPERTIES

Composition of concrete (2)

Water - cement ratio	.35
Aggregate - cement ratio	3.5
Water content (kg/m^3)	170
Cement content (kg/m^3)	500
Slump (mm)	40-60
Design strength (MPa)	45

Composition of aggregate (2)

Aggregate	Percent by weight	Weight of aggregate kg/m^3
Nom. 19 mm	59	1020
Nom. 9.5 mm	11	195
Coarse sand	23	400
Fine sand	7	120

Combined aggregate grading (2)

Sieve size (mm)	Cumulative percent passing
26.5	100
19.0	100
13.2	69
9.5	46
4.75	32
2.36	31
1.18	22
0.60	14
0.15	3
0.075	1

Petrographic analysis fo the 19 mm nominal size aggregate (2)

Rock type	Percent by weight
Quartzose (Quartz, Jasper, Chert, Quartizite)	82.5
Hornfels	7.4
Volcanics	5.0
Sediments	5.1

APPENDIX II - IMPLEMENTATION OF THE CEB RECOMMENDATIONS FOR THE DEFERRED DEFORMATIONS (3)

The code assumes that the total deformation due to creep is composed of two parts: the reversible part (delayed elasticity) and the irreversible part (flow). In addition, the code assumes that the irreversible part has a large component during the first day after loading and this is represented in the form of an additional term. The Code also requires the time to be adjusted to take account of the maturity of concrete which is a function of temperature and age of hardening.

The incremental creep strain at time t under constant load applied to time t_o is given by:

$$\varepsilon_c (t,t_o) = \frac{\sigma_o \phi(t,t_o)}{EC28}$$

where t and t_o are the adjusted times, σ_o is the constant stress and EC28 is the modulus of elasticity of concrete at 28 days, and $\phi(t,t_o)$ is the creep coefficient.

The creep coefficient includes the three part creep deformation, namely:

$$\phi(t,t_o) = \beta_a(t_o) \quad \text{single component of the irreversible deformation}$$

$$+ \phi_f \left[\beta_f(t) - \beta_f(t_o)\right] \quad \text{irreversible component}$$

$$+ \phi_d \, \beta_d(t - t_o) \quad \text{reversible component which uses real non-adjusted time.}$$

The adjusted time is given by the following empirical formula:

$$t = \frac{1}{30} \sum_{o}^{t_m} \left\{\left[T(t_m) + 10\right] \Delta t_m\right\}$$

Where t_m - real age of concrete in days, T - average daily temperature of the concrete in degrees Celsius, Δt_m - the number of days when the average daily temperature has assumed the value T.

For the investigated girder the adjusted time was calculated as follows (see Table 1 for the time-table):

- first two hours after pouring at normal temperature of 21°C $(21 + 10) \times \frac{2}{24}$
- twelve hours of curing at an average temperature of 75°C $(75 + 10) \times \frac{12}{24}$
- seven hours of cooling at an average temperature of 30°C $(30 + 10) \times \frac{7}{24}$

The adjusted time up to the end of curing:

$$\frac{1}{30 \times 24}\left[31 \times 2 + 85 \times 12 + 40 \times 7\right] = 1.85 \text{ days}$$

While the real time is 21/24 = 0.875 days, the difference being around 1 day. For the sake of simplicity the adjusted time of the end of curing was rounded off to two days. It is important to remember that end of curing corresponds also to the time of loading, hence t_o = 2 days. After the end of curing, the seasonal temperatures were such, that it was reasonable to assume 21°C as daily average and this temperature did not require any adjustment.

For the adjusted time of two days the single component of the irreversible deformation

$$\beta_a(t_o) = 0.8\left(1 - \frac{\text{concrete strength at 2 days}}{\text{concrete strength at } t = \infty}\right)$$

Therefore using Table 2

$$\beta_a(t_o) = 0.8\left(1 - \frac{36.6}{51.3}\right) = 0.23$$

The coeffiecient of the irreversible deformation is given by

$$\phi_f = \phi_{f1} \times \phi_{f2}$$

where ϕ_{f_1} depends on the moisture in the ambient environment. Since no record of daily humidity was available it has been assumed that the relative humidity varied between 50% and 80%. This corresponds to ϕ_{f_1} varying between 2.67 and 1.5. ϕ_{f_2} depends on notional thickness h_o.

$$h_o = \lambda \frac{2A_c}{u}$$

where λ is a coefficient which depends on ambient environment and for this range of humidities varies between 3.25 and 1.30, A_c is the area of gross concrete section (A_c = 0.5123 m) u is the perimeter in contact with atmosphere (in this case the whole perimeter) u = 4.554 m.

Using these values h_o varies between 731 mm and 299 mm which are rounded off to 800 mm and 300 mm.

The range of numerical coefficients ϕ_{f_1}, ϕ_{f_2} and ϕ_f is summarised below:

Percent daily humidity	λ	h_o mm	ϕ_{f_1}	ϕ_{f_2}	ϕ_f	ϕ_f rounded off
50	1.30	300	2.67	1.47	3.92	4.0
80	3.25	800	1.50	1.25	1.88	2.0

$\beta_f(t)$ is given as function of the adjusted time and of the notional thickness. $\beta_f(t)$ for h_o = 300 was averaged between $\beta_f(t)$ corresponding to h_o = 400 and 200 mm.

The coefficient of the reversible component ϕ_d has a constant value of 0.4 and β_d is given as a single function of the real time difference $(t - t_o)$. EC28 was taken from Table 2 and multiplied subsequently by 1.1 to take account of the prestressed reinforcement.

Shrinkage strain is given as a multiplication of the basic shrinkage coefficient multiplied by the time-dependent functions β_s. Both the coefficient and β_s depend on ambient humidity directly or via h_o.

The shrinkage strain $\varepsilon_s(t,t_o)$ equals:

$$\varepsilon_s(t,t_o) = \varepsilon_{so}\left[\beta_s(t) - \beta_s(t_o)\right]$$

where $$\varepsilon_{so} = \varepsilon_{s1} \times \varepsilon_{s2}$$

Values of ε_{so} for two different percentages of humidity are given below:

Percent daily humidity	h_o mm	ε_{s1}	ε_{s2}	ε_{so}	ε_{so} rounded off
50	300	0.000443	0.85	0.000377	0.0004
80	800	0.00025	0.77	0.000193	0.0002

APPENDIX III - COMPARISON WITH AUSTRALIAN STANDARD AS-1481 (1)

The expected magnitudes of creep at a particular time as calculated from CEB data are compared below with expected magnitudes of creep as calculated from AS-1481.

AS-1481

The creep coefficient $\phi(t,t_o)$ is given as multiplication of four coefficients

$$\phi(t,t_o) = k_c \times k_d \times k_e \times k_h$$

where k_c depends on relative humidity, k_d depends upon the degree of hardening at time of loading, k_e depends on theoretical thickness of the section, k_h depends on the development of creep with time.

Theoretical thickness $= \frac{2A_c}{\mu} = 225$ mm

k_c = 1.4 for 50% relative humidity and
0.8 for 80% of relative humidity.

k_d = 1.8

k_e = 0.783

k_h = 0.09 for 10 days

k_h = 0.3625 for 100 days

Humidity	$k_d \times k_e \times k_h$	k_c	$\phi(t,t_o)$	
50%	0.13	1.4	0.18	at 10 days
80%	0.13	0.8	0.10	
50%	0.51	1.4	0.72	at 100 days
80%	0.51	0.8	0.41	

The corresponding CEB creep coefficients are (see Appendix II):

Time dependent component	at 10 days		at 100 days	
	Humidity		Humidity	
	50%	80%	50%	80%
$\beta_f = \beta_f(t) - \beta_f(t_o)$	.188	.16	.4265	.395
$\beta_d = \beta_d(t - t_o)$	.405	.405	.69	.69

$\phi(t,t_o) = \beta_a + \phi_f \beta_f + \phi_d \beta_d$

Humidity	β_a	ϕ_f	β_f	ϕ_d	β_d	$\phi(t,t_o)$	
50%	.23	3.92	.188	.4	.405	1.13	at 10 days
80%	.23	1.88	.16	.4	.405	.69	
50%	.23	3.92	.4265	.4	.69	2.18	at 100 days
80%	.23	1.88	.395	.4	.69	1.25	

$\phi(t,t_o)$ for $\beta_a = 0$

Humidity	$\phi(t,t_o)$	
	at 10 days	at 100 days
50%	0.9	1.95
80%	0.46	1.02

APPENDIX IV - REFERENCES

1. AUSTRALIAN STANDARD 1481-1978. "SAA Prestressed Concrete Code", Standards Association of Australia.

2. CARSE, A. "Static Chord Modulus of Elasticity of High Strength Concrete in Uniform Compression and Flexure", (Qld). Thesis for the M.Eng.Sc. in Engineering, 1979.

3. CEB-FIP, "Model Code for Concrete Structures", 1978.

4. ENGLAND, G.L. "Numerical Creep Analyses Applied to Concrete Structures", J. of the ACI, June, 1967, pp 301-312.

5. CHURCHWARD, A.J. and SOKAL, Y.J. "Temperature Effects in a Concrete Bridge Superstructure", 7th A'asian Conference on Mechanics of Structures and Material, Univ. of Western Australia, 1980, pp 73-79.

6. ILLSTON, J.M. "Components of Creep in Mature Concrete", J. of the ACI, March, 1968, pp 219-228.

7. KORETSKY, A.V. and PRITCHARD, R.W. "Study of Relaxation Losses in 12.5 mm diameter Super Grade Low Relaxation Strands", 10th ARRB Conference, Univ. of Sydney, 1980, pp 71-78.

8. MORRISON, V. and GAMBLE, W.L. "Time Dependent Behaviour of Noncomposite and Composite Prestressed Concrete Structures under Field and Laboratory Conditions", Structural Research Series No. 385, Univ. of Illinois, 1972, p 517.

9. ROSS, A.D. "Creep of Concrete under Variable Stress:, J. of ACI, March, 1958, pp 739-758.

10. SANCHEZ-GALVEZ, V., ELICES, M., ERDELYI, A., and KOSIOREK, M. "Stress Relaxation Due to Steam Curing", Meteriaux et Constructions, Vol. 10, No. 60, 1977, pp 351-356.

11. VAN HERBERGHEN, P.L., LAMBOTTE, H., and VAN ACKER, A. "Etude des Pertes de Precontrainte pour Relaxation de l'Acier sous l'Influence d'un Cycle d'Etuvage", Congres International FIP, New York, 1974, p 25.

12. McEVOY, J., and TYRER, P. "Time-Dependent Camber of a Prestressed Concrete Girder", Thesis presented to the Department of Civil Engineering, Univ. of Queensland in partial fulfillment of the requirements for the degree of Bachelor of Engineering, 1979.

APPENDIX V - NOTATION

Symbol	Meaning
A_c	area of gross concrete section
EC28	modulus of elasticity of concrete in compression measured on 28th day after casting
h_o	notional thickness
k_c, k_d, k_e, k_h	coefficients in the calculation of deformation from creep and shrinkage
N	digital counter
R	loss of stress from relaxation
t	time
t_m	age of concrete
t_o	initial time
T	temperature
$\beta_d(t)$	reversible component in creep strain at time t
$\beta_f(t)$	irreversible component in creep strain at time t
$\beta_s(t)$	component in shrinkage strain at time t
$\beta_a, \beta_d, \beta_f$	coefficients in the calculation of creep strain
Δt_m	time interval
$\varepsilon_c(t,t_o)$	total creep strain at time t initiated at time t_o
$\varepsilon_s(t,t_o)$	total shrinkage strain at time t initiated at time t_o
$\varepsilon_{so}, \varepsilon_{s1}, \varepsilon_{s2}$	shrinkage strain coefficients
λ	coefficient in the calculation of notional thickness
μ	perimeter of the section in contact with atmosphere
σ_o	the applied constant stress
$\phi(t,t_o)$	creep coefficient = ratio between creep strain at time t and elastic strain at time t_o
$\phi_f, \phi_{f1}, \phi_{f2}, \phi_d$	coefficients in the calculation of creep strain

CIVIL ENGINEERING RESEARCH REPORTS

CE No.	Title	Author(s)	Date
20	Consolidation of Axi-symmetric Bodies Subjected to Non Axi-symmetric Loading	CARTER, J.P. & BOOKER, J.R.	January, 1981
21	Truck Suspension Models	KUNJAMBOO, K.K. & O'CONNOR, C.	February, 1981
22	Elastic Consolidation Around a Deep Circular Tunnel	CARTER, J.P. & BOOKER, J.R.	March, 1981
23	An Experimental Study of Blockage Effects on Some Bluff Profiles	WEST, G.S.	April, 1981
24	Inelastic Beam Buckling Experiments	DUX, P.F. & KITIPORNCHAI, S.	May, 1981
25	Critical Assessment of the International Estimates for Relaxation Losses in Prestressing Strands	KORETSKY, A.V. & PRITCHARD, R.W.	June, 1981
26	Some Predications of the Non-homogenous Behaviour of Clay in the Triaxial Test	CARTER, J.P.	July, 1981
27	The Finite Integral Method in Dynamic Analysis : A Reappraisal	SWANNELL, P.	August, 1981
28	Effects of Laminar Boundary Layer on a Model Broad-Crested Weir	ISAACS, L.T.	September, 1981
29	Blockage and Aspect Ratio Effects on Flow Past a Circular Cylinder for $10^4 < R < 10^5$	WEST, G.S. & APELT, C.J.	October, 1981
30	Time Dependent Deformation in Prestressed Concrete Girder: Measurement and Prediction	SOKAL, Y.J. & TYRER, P.	November, 1981
31	Non-uniform Alongshore Currents and Sediment Transport - a One Dimensional Approach	GOURLAY, M.R.	January, 1982
32	A Theoretical Study of Pore Water Pressures Developed in Hydraulic Fill in Mine Stopes	ISAACS, L.T. & CARTER, J.P.	February, 1982

CURRENT CIVIL ENGINEERING BULLETINS

4 *Brittle Fracture of Steel — Performance of ND1B and SAA A1 structural steels: C. O'Connor (1964)*

5 *Buckling in Steel Structures — 1. The use of a characteristic imperfect shape and its application to the buckling of an isolated column: C. O'Connor (1965)*

6 *Buckling in Steel Structures — 2. The use of a characteristic imperfect shape in the design of determinate plane trusses against buckling in their plane: C. O'Connor (1965)*

7 *Wave Generated Currents — Some observations made in fixed bed hydraulic models: M.R. Gourlay (1965)*

8 *Brittle Fracture of Steel — 2. Theoretical stress distributions in a partially yielded, non-uniform, polycrystalline material: C. O'Connor (1966)*

9 *Analysis by Computer — Programmes for frame and grid structures: J.L. Meek (1967)*

10 *Force Analysis of Fixed Support Rigid Frames: J.L. Meek and R. Owen (1968)*

11 *Analysis by Computer — Axisymetric solution of elasto-plastic problems by finite element methods: J.L. Meek and G. Carey (1969)*

12 *Ground Water Hydrology: J.R. Watkins (1969)*

13 *Land use prediction in transportation planning: S. Golding and K.B. Davidson (1969)*

14 *Finite Element Methods — Two dimensional seepage with a free surface: L.T. Isaacs (1971)*

15 *Transportation Gravity Models: A.T.C. Philbrick (1971)*

16 *Wave Climate at Moffat Beach: M.R. Gourlay (1973)*

17. *Quantitative Evaluation of Traffic Assignment Methods: C. Lucas and K.B. Davidson (1974)*

18 *Planning and Evaluation of a High Speed Brisbane-Gold Coast Rail Link: K.B. Davidson, et al. (1974)*

19 *Brisbane Airport Development Floodway Studies: C.J. Apelt (1977)*

20 *Numbers of Engineering Graduates in Queensland: C. O'Connor (1977)*